Scale up study of capillary microreactors in solvent-free semihydrogenation of 2-methyl-3-butyn-2-ol

Nikolay Cherkasov[a], Ma'moun Al-Rawashdeh[a], Alex O. Ibhadon[b], Evgeny V. Rebrov[a,c*]

[a] School of Engineering, University of Warwick, Library Road Coventry, CV4 7AL, United Kingdom

[b] Catalysis and Reactor Engineering Research Group, Department of Chemistry and School of Biological, Biomedical and Environmental Sciences, University of Hull, Cottingham Road, Hull, HU6 7RX, United Kingdom

[c] Department of Biotechnology and Chemistry, Tver State Technical University, Tver, 170026, Russia

(*Corresponding Author's E-mail: e.rebrov@warwick.ac.uk)

ABSTRACT

A 2.5 wt. % Pd/ZnO catalytic coating deposited unto the inner wall of a capillary reactor with a diameter of 0.53 and 1.6 mm was characterised by XRD, SEM, TEM and elemental analysis. The performance of catalytic reactors was studied in solvent-free hydrogenation of 2-methyl-3-butyn-2-ol. No mass transfer limitations were observed in the reactor with a diameter of 0.53 mm up to a catalyst loading of 1.0 $kg_{(Pd)}$ m^{-3}. The activity and selectivity of the catalysts have been studied in a batch reactor to develop a kinetic model. This model was combined with a reactor model to describe the obtained data in a wide range of reaction conditions. The model was applied to calculate the range of reaction conditions required to obtain a production rate of liquid product of 10-50 kg a day in a single catalytic capillary reactor.

Keywords: Semihydrogenation; catalytic coatings; microreactor; Palladium; alkynol.

1. Introduction

Process safety and small environmental footprint are one of the main challenges of chemical industry, and microreactors seem to be one of the most promising technologies. Small dimensions of microreactors provide large surface to volume ratio, orders of magnitude higher than that of conventional reactors, and result in high heat and mass transfer rates [1–4]. Quick mass transfer opens up new ways for improved product selectivity by avoiding mass and heat transfer limitations which eliminate hot spots that generally lead to over-reaction, catalyst deactivation and rise safety concerns. Another important benefit of microreactors lies in the ability to use high reaction temperature and pressure without compromising on the process safety. Even in the case of catastrophic reactor malfunction only very small amount of harmful substances will be released due to the low liquid hold up [5]. Because of intrinsic safety and excellent reaction control, microreactors can be utilised under reaction conditions that are prohibited for large-scale reactors. This opens new operational regimes and substantial process intensification capabilities [6–8]. An important societal advantage of safer microreactor processes is the synthesis on demand on a smaller scale at the place where products are needed, the approach which decreases concentration of industrial units and reduces transportation costs [7].

Microreactor technology has been successfully used in a number of processes both in academia and in industry [9–12]. The advantages of microreactors have been clearly demonstrated for non-catalytic gas-liquid and liquid-liquid reactions that require precise control over reaction conditions, or involve dangerous chemicals such as corrosive fluorine or explosive diazo-compounds [13–16]. However, considering that the vast majority of modern chemical processes utilise heterogeneous catalysts to replace stoichiometric reactions due to obvious economic and environmental advantages, the application of catalytic coatings in microreactors is disproportionately scarcely studied [17]. A few gas-phase heterogeneously catalysed reactions have been studied in various reactions such as Fisher-Tropsch synthesis, CO_2 hydrogenation, water gas shift [18], preferential CO oxidation [19], and complete oxidation of organic compounds [20] demonstrating a 2-5 fold increase in reaction rates compared to conventional reactors [21–24].

However, the class of heterogeneously-catalysed multiphase (liquid-liquid or gas-liquid) reactions received limited attention because of the difficulty to precisely control catalyst-substrate interactions. The reactions can be performed either using a (i) catalyst particles in a micro fixed bed configuration [2,25], (ii) magnetically-supported catalysts held at the reactor walls with magnetic field [26–29], (iii) introducing a slurry of solid catalyst particles into the reactant flow [30], (iv) catalytic wall coatings obtained via hydrothermal synthesis [31,32] or methods derived

from dipcoating, spincoating or washcoating [33–39]. Micro fixed bed reactors with a typical pellet size below 100 μm seem to offer a simple way of catalyst introduction and they are suitable for any catalyst. However, catalytic beds have a number of problems such as bed densification with time resulting in considerable pressure build-up which requires catalyst dilution with a hard inert material. Also, the removal of heat from the reaction zone to the external walls could create considerable radial gradients in the reactor in a highly exothermic reaction. Finally, liquid channelling may result in very wide residence time distribution and therefore poor product selectivity in consecutive reactions [40–42]. However, for a limited class of reactions that have no side products, packed-bed reactors can successfully be applied [5,40]. Magnetically-recoverable catalysts offer a convenient way of catalyst introduction and separation, but their benefits are counterbalanced by more complex reactor design required [43–45]. A slurry of solid catalyst particles can be introduced into a liquid stream and provides good selectivity towards intermediate products which is comparable to that of an ideal stirred-tank reactor [30]. However, this approach requires an additional expensive step to separate catalysts from the reaction products. Also the reactant to catalyst ratio is much lower compared to other reactor types in order to provide good catalyst distribution and high conversion. Wall coated capillary reactors combine simplicity of operation and high throughput with excellent reaction control which lead to high selectivity towards intermediate products [33,34,46]. Their synthesis methods have been considerably improved over the last decade and very stable catalytic coatings were obtained for a range of industrial applications following a recently developed synthesis method [33].

There exists a limited number of publications describing the upscaling of catalytic capillary microreactors [47,48]. While the numbering up approach looks very promising to increase the throughput, it might require 10^2-10^5 parallel channels to produce 1-100 ton of product per year. The exact number of microchannels depends on the maximum allowed pressure drop over the reactor and the channel length which is often limited by available microfabrication methods [49–52]. Therefore the numbering up approach needs to be combined with scaling up of the reactor dimensions to bring the throughput to the industrial scale while avoiding mass or heat transfer limitations.

The aim of the work was to study the feasibility of carrying out industrially-relevant semihydrogenation reactions in wall-coated capillary microreactors and investigate the feasibility of reactor upscaling in order to obtain the desired production capacity. In this study, selective hydrogenation (semihydrogenation) of 2-methyl-3-butyn-2-ol (MBY) over a Pd/ZnO catalyst was chosen as a model reaction representing a wide class of important gas-liquid reactions catalysed by a supported heterogeneous catalyst. The replacement of traditional batch reactors with slurry catalysts by catalytic capillary microreactors is expected to provide (i) substantial safety benefits

due to minimisation of explosive hydrogen utilisation and (ii) decreased labour costs due to quick process optimisation.

2. Experimental

2.1. Reactor preparation and characterisation

Two groups of capillary reactors were used: (i) fused silica capillary microreactors with an internal diameter of 0.53 mm and a length of 1 m, and (ii) glass tubes millireactors with an internal diameter of 1.6 mm, and a length of 0.2 m. The reactors are further referred to as r0.53-xx, where 0.53 is the internal diameter in mm and xx is the total Pd loading in kg $m^{-3}_{(reactor)}$. A 2.5 wt.% Pd/ZnO catalytic coating was deposited onto the inner reactor walls following the previously reported method [33]. The sol containing catalyst precursors was introduced into the capillary reactors and the solvent was evaporated by moving the capillary into the oven at 200 ^{o}C at the displacement speed of 0.3 mm s^{-1}. The coating thickness was varied from 2 to 65 μm by adjusting the number of coatings cycles and the concentration of precursors in the initial sol. The surfactants were removed by heating the coated reactor in a vacuum oven (1 mbar residual pressure) at 200 ^{o}C overnight. After cooling to room temperature, the reactors were consecutively flushed with water and acetone (1 mL min^{-1}, 10 min each) followed by drying in air.

Many coated reactors were cut and glued on a microscope stubs with epoxy. Then many (typically 6-9) cross-sections from every reactor were studied on a TM-1000 Hitachi scanning electron microscope (SEM) in a high-pressure mode to minimise charging without deposition of an additional conductive coating. Ttransmission electron microscopy (TEM) images of the coatings were obtained using a Jeol 2010 transmission electron microscope equipped with an energy-dispersive X-ray spectrometer (EDX, Oxford Instruments). The study was performed from 5-8 different regions to obtain representative data. In this study, the coating from the reactors was removed, dispersed in ethanol under sonication and a few droplets of the dispersion were dropped on a carbon-coated copper grid.

Powder X-ray diffraction, (XRD), measurements were performed using an Empyrean X-ray diffractometer equipped with monochromatic Kα-Cu X-ray source and a PIXcel linear detector. The scanning was performed in a stepwise mode within a 2θ range of 20-85^{o} with a step length of 0.0390^{o} 2θ, and a step time of 60 min studying the coating removed from the capillaries on a zero background sample holder.

After the reaction, the total catalyst loading in the capillaries was determined dissolving the coating by withdrawing 1 mL of aqua regia (1:3 volume mixture of concentrated HCl and HNO_3, Sigma-Aldrich) at 0.4 mL min^{-1} through the capillaries. The resulting solution was collected in a

5 mL volumetric flask and diluted with deionised water. The solutions were studied using a Perkin Elmer Optima 5300DV emission inductively coupled plasma spectrometer.

2.2. Capillary reactor testing

The experimental setup consists of a continuous flow syringe pump fed with MBY (Sigma-Aldrich, > 98 wt. %) without solvent, mass flow controllers and a pressure transducer connected via an X-joint to the capillary reactor (Figure 1). The reactor was placed into a thermostatic water bath at the temperature of 70.0 ±0.4 °C. The reactor outlet was connected to an automatic sample collector via an additional silica capillary (i.d. 250 µm) that provided a pressure drop of 0.20±0.03 bar. The liquid samples were diluted 100:1 with hexane and analysed using a Varian 430 gas chromatograph equipped with a 30 m Stabiwax capillary column and a flame ionisation detector.

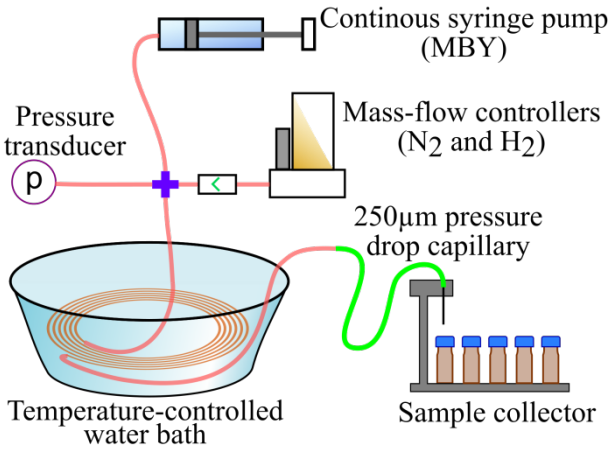

Figure 1. Scheme of the capillary reactor setup.

2.3. Reference catalyst synthesis

A reference Pd/ZnO powder catalyst synthesised by a conventional polyol method [53]. was used for kinetic study in a batch reactor. s A powder of ZnO, 2 g, particle sizes < 20 µm (Alfa Aesar), was added to a solution of palladium acetate (>99 wt. %, Sigma-Aldrich) in 50 mL ethylene glycol (>99 wt. %, Sigma-Aldrich). The amount of palladium precursor was adjusted to obtain a 2 wt. % Pd/ZnO catalyst. The dissolved air was displaced with a nitrogen flow of 100 mL min^{-1} followed by reflux heating for 2 h. Then, the solution was centrifuged, washed with water (2x30 mL), acetone (2x30 mL) and dried in nitrogen. The catalyst was characterised by N_2 adsorption and TEM. The complete reduction of Pd was confirmed by elemental analysis data.

2.4. Batch reactor testing

Hydrogenation in a batch reactor at atmospheric pressure was performed in a 10 mL two-neck round bottom flask equipped with a water-cooled condenser, and a septum for gas

introduction and liquid withdrawal. The 2 wt. % Pd/ZnO reference catalyst (30.0 mg) was added to 4.0 mL of MBY without any additional solvent. The reaction mixture was stirred using a magnetic stirrer. The stirring rates were in the range of 600 – 1200 rpm. The reaction temperature was controlled with a water bath at 70.0±0.1 ^{o}C. The gases were introduced to the bottom of the reactor via a 250 μm id silica capillary and the flow rates were controlled by mass-flow controllers. The reactor was flushed with a flow of 20 mL min^{-1} of nitrogen (99.999 vol.%, BOC) for 10 min to remove air, then hydrogen was quickly introduced at a flow of 50 mL min^{-1} for 1 min to displace nitrogen. Afterwards, the reaction was performed feeding a hydrogen flow of 15 mL min^{-1} through the reaction mixture and withdrawing 20 uL of the reaction mixture regularly for off-line analysis. The absence of mass transfer limitations was confirmed by studying the reaction rate at various stirring speeds and catalyst amounts. The liquid samples were diluted 100:1 with heptane and analysed using a Shimadzu 2010 gas chromatograph equipped with a Stabiwax capillary column and a flame ionisation detector.

3. Results and Discussion

3.1. Characterisation of the capillary reactors

Figure 2 shows representative SEM images of catalytic coatings in the r0.53 reactors. No continuous ZnO layer was obtained at the catalyst loading corresponding to the Pd content below 0.7 kg(Pd) m_r^{-3}. These coatings consisted of separate particles of Pd/ZnO deposited onto the reactor walls (Figure 2 a,b). Statistical analysis of the coating in 5 capillary reactors with the Pd loading below 0.7 kg(Pd) m_r^{-3} shows that the dimensions of catalytic particles are independent of total Pd content and are about 2.3±2.0 μm (average value ± standard deviation). Likely, the formation of individual particles was caused by capillary forces of the evaporating solvent. At a higher catalyst content, however, the capillary was coated with a rather uniform catalytic layer with a thickness of 11.9±6.0 μm. The coating consisted of ZnO crystallite platelets which formed cavities with a characteristic size in the micrometer range (Figure 2c, d).

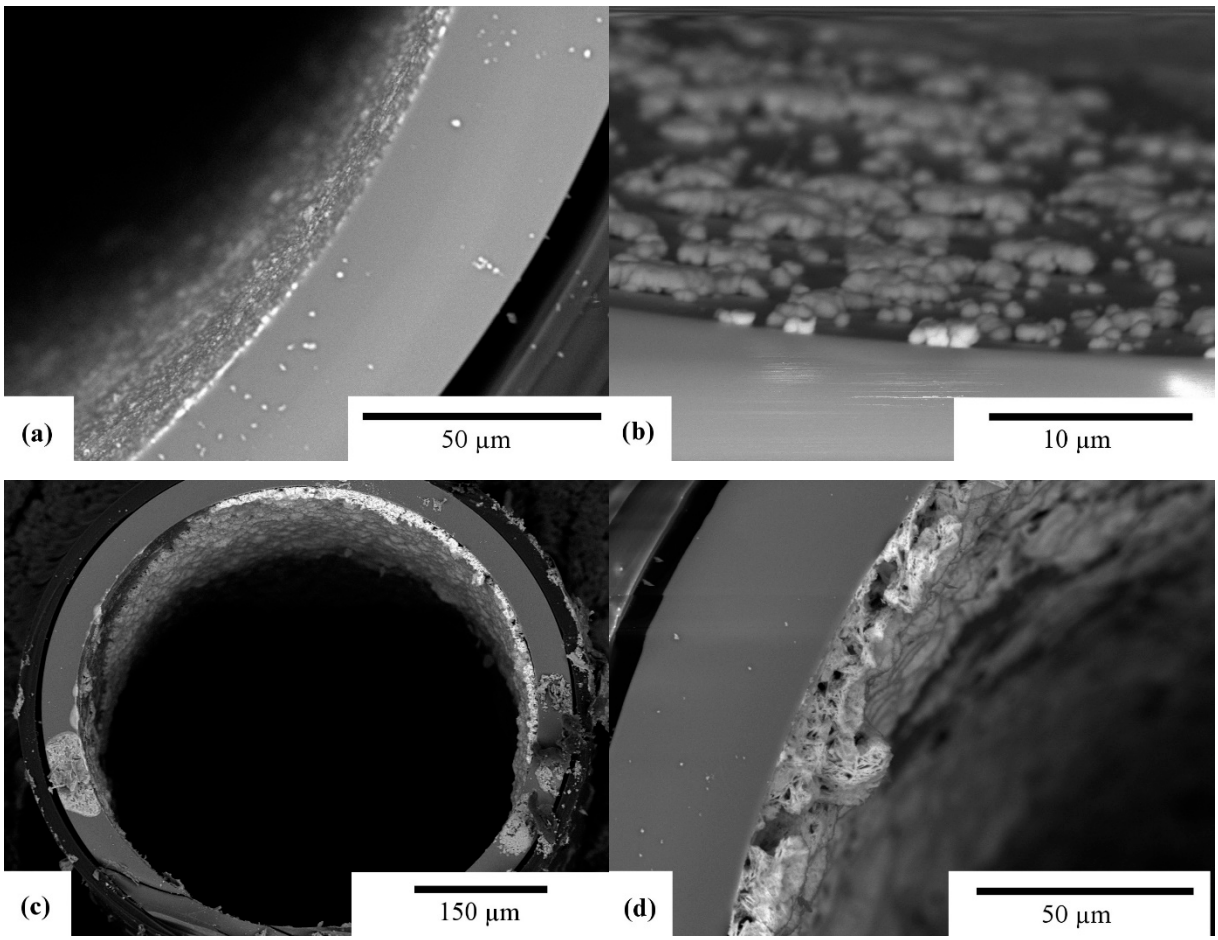

Figure 2. Cross sectional SEM photographs of the 0.53 mm i.d. capillary reactors wall-coated with Pd/ZnO, total Pd content is (a) 0.24, (b) 0.64, (c, d) 2.35 kg (Pd) m^{-3}(reactor).

SEM study of various r1.6 reactors showed that the coating was not uniform at the catalyst loading below 0.7 kg(Pd) m_r^{-3}. The coating consisted of individual ZnO particles with a mean size of 6.7±5.2 μm. At a higher catalyst content, a uniform coating was obtained onto the reactor walls with the thickness increasing from 36±22 to 65±30 μm for the r1.6-1.0 and r1.6-1.8 reactors, respectively. A Pd loading in all the capillary reactors of 2.53±0.37 wt. % was determined by EDX analysis. This value is in a good agreement with the nominal Pd loading of 2.5 wt. %. This demonstrates that no Pd was lost during the coating and washing process.

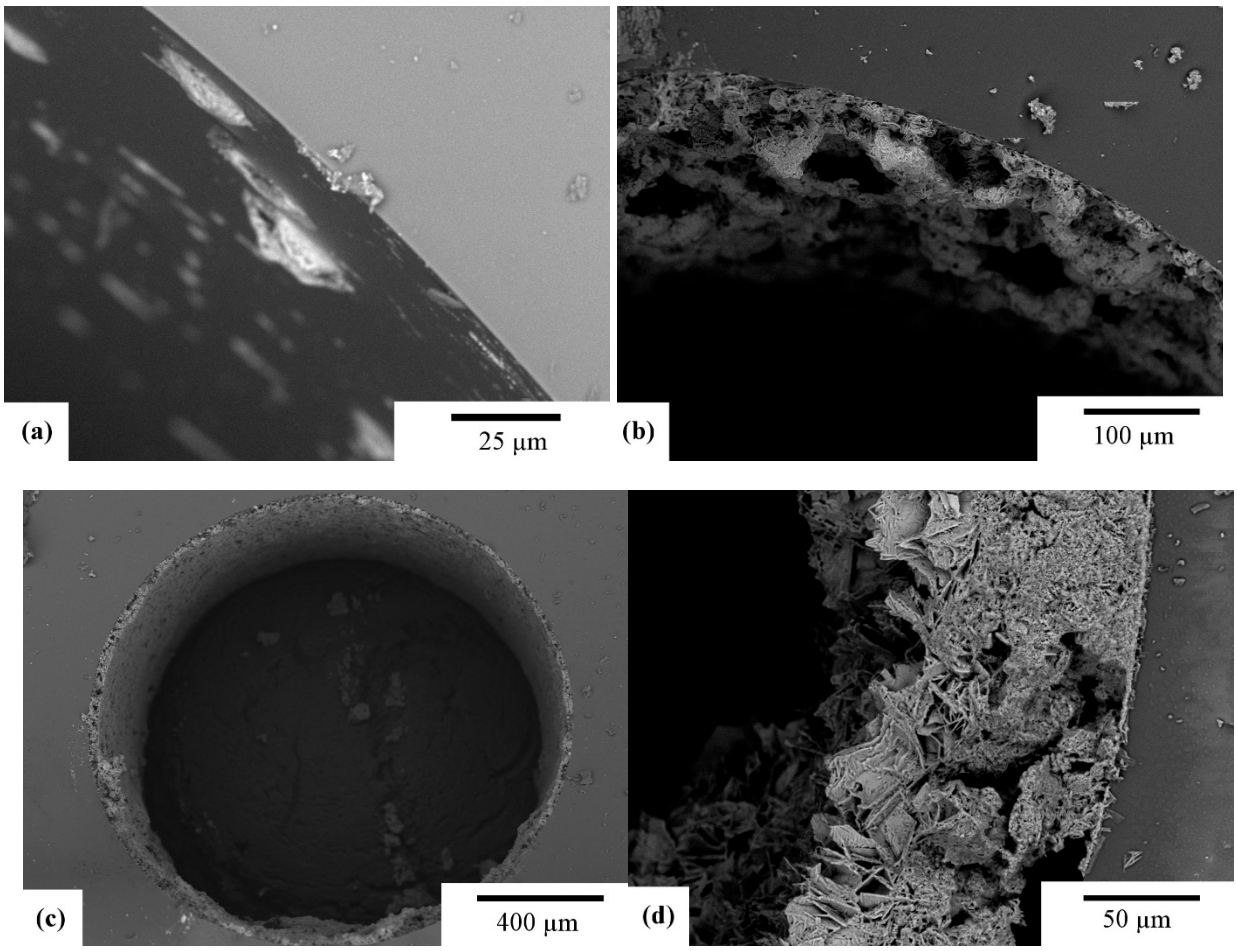

Figure 3. Cross sectional SEM photographs of the 1.6 mm i.d. capillary reactors wall-coated with Pd/ZnO, total Pd content is (a) 0.17, (b) 1.03, (c) 1.23, (d) 1.76 kg (Pd) m^{-3}(reactor).

The powder XRD pattern of the Pd/ZnO catalyst (Figure 4) showed that wurtzite was the only ZnO phase in the coatings. Its crystallite size was estimated using Scherrer's formula to be about 30 nm. This is a typical size obtained in the developed sol-gel method after a calcination step at 200 ºC as low calcination temperature prevents sintering of ZnO nanoparticles. A small Pd peak is present at 40º 2θ.

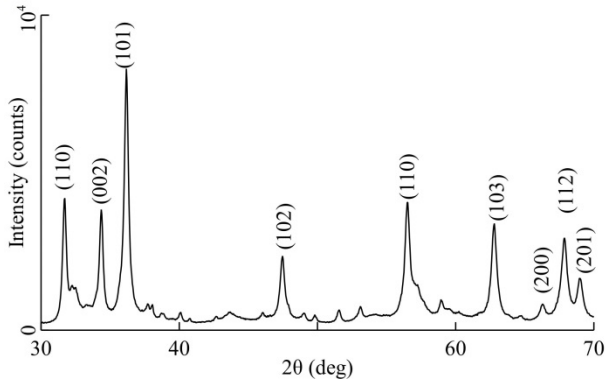

Figure 4. Powder X-ray diffraction pattern of the Pd/ZnO catalytic coating extracted from a millireactor.

Figure 5 shows a characteristic TEM image of a coating detached from the r1.6-1.0 reactor. It can been seen in Figure 5 that the Pd particles with a mean size of 3.0±1.0 nm are evenly distributed through the ZnO framework. These particles are formed by several smaller nanoparticles about 1.3 nm in diameter. The morphology and dimensions of Pd nanoparticles were the same for r0.53 and r1.6 capillary reactors.

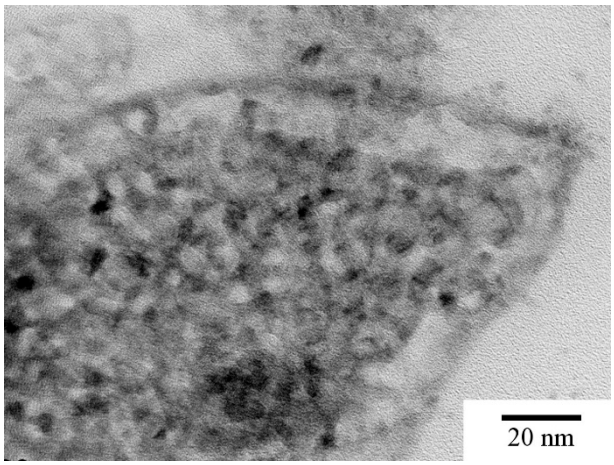

Figure 5. A representative TEM microphotograph of the Pd/ZnO coating removed from the r1.6-1.0 reactor.

3.2. Semihydrogenation in capillary reactors

Two series of capillary reactors, r0.53 and r1.6, were studied in solvent-free MBY hydrogenation. The conditions were selected to ensure that the conversion of MBY was below 80 %, which allowed for determination of apparent reaction rates directly from MBY conversion as the reaction rate follows a pseudo-zero order kinetics [54,55]. The alkene selectivity above 97.5 % was observed for all the reactors studied except for the r1.6-1.8 reactor. These data show that there were no internal diffusion limitations of MBY or liquid channelling that usually substantially decrease selectivity.

It can be seen in Figure 6, that the MBY conversion in r0.53 reactors with different Pd loadings was linearly proportional to the catalyst loading up to a Pd content of 0.75 kg m^{-3} at a liquid flow rate of 10 µL min^{-1}. This confirms the absence of mass transfer limitations. At a higher Pd loading of 2.4 kg m^{-3}, the full MBY conversion was observed therefore the flow rates was increased to 40 µL min^{-1} to get kinetic data. At the higher flow rate, the MBY conversion increased linearly with catalyst loading up to a Pd content of 0.7 kg m^{-3}. At a higher Pd loading of 2.4 kg m^{-3} the reaction rate was affected by the onset of mass-transfer limitations. For the r1.6 reactors, similarly, the MBY conversion was proportional to the Pd loading in the whole range of Pd loadings studied.

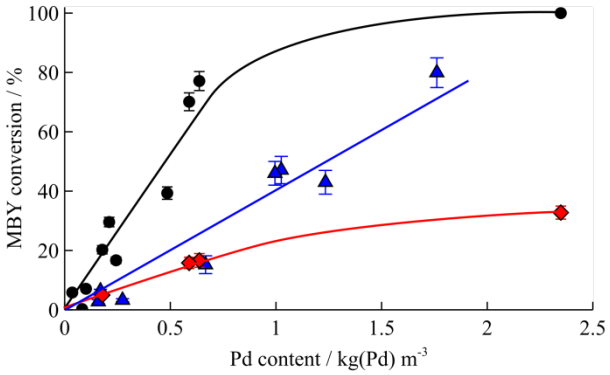

Figure 6. MBY hydrogenation over a Pd/ZnO catalytic coating in (■,♦) r0.53 (0.53 mm i.d). and (▲) r1.6 (1.6 mm i.d.)capillary reactors. Liquid flow rate: (■,▲) 10 µL min^{-1} or (♦) 40 µL min^{-1}, reaction temperature: 70 C, H_2 flow rate: 10 mL min^{-1} (STP), absolute reaction pressure 1.2 bar.

The reactant conversion in a zero-order catalytic reaction is proportional to the amount of catalyst in the reactor, the fraction of the total reactor volume occupied by the liquid (which is determined by the liquid hold up) and inversely proportional to the liquid reactant flow rate. The zero-order reaction kinetics is described by Eq. 1:

$$C_{MBY} = C^0_{MBY}(1 - k_0^{'}\ \tau_{res}\ ) \qquad (1),$$

where τ_{res} is the liquid residence time ($\tau_{res} = \frac{V_{cat}}{F_V}\varepsilon_L$), V_{cat} is the catalyst volume, ε_L is the liquid hold-up in the reactor, and F_v is the volumetric liquid flow rate, and $k_0^{'}$ is the pseudo zero-order reaction rate constant. Eq. 1 can be rearranged in terms of MBY conversion (X_{MBY}):

$$X_{MBY} = k_0^{'}\ \tau_{res} \qquad (2)$$

Figure 7 shows the change in reactant concentration as a function of residence time. It can be seen that no mass transfer limitations were observed for the r0.53 up to the catalytic loading of 1 kg(Pd) m_r^{-3}. For the r1.6 reactors, the observed rates were lower than that in the r0.53 reactors suggesting the presence of mass transfer limitations.

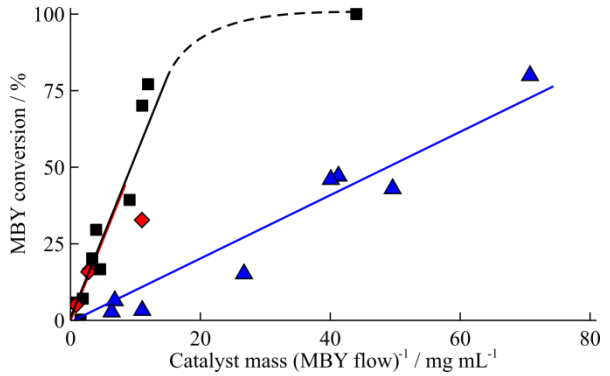

Figure 7. MBY conversion in r0.53 and r1.6 reactors. The conditions and notations are the same as those in Figure 6.

3.3. Semihydrogenation in a batch reactor

The MBY semihydrogenation was performed using a 2 wt. % Pd/ZnO catalyst in a batch reactor. The reaction rate was independent on the stirring speed above 900 rpm confirming the absence of mass transfer limitations. The catalyst was non-porous with a specific surface area of 4.1 m^2 g^{-1}. The Pd nanoparticles were 3.2 ±1.1 nm according to TEM data (not shown). The Pd dispersion in the model catalyst was the same as that in the catalytic coatings which allowed direct data comparison between the model catalyst and catalytic coatings.

The reaction kinetics was modelled to explain the difference in the performance between r0.53 and r 1.6 reactors. The MBY hydrogenation reaction scheme (Figure 8) consists of three main reactions: (i) MBY hydrogenation to MBE followed by (ii) MBE hydrogenation to MBA and (iii) a direct hydrogenation step of MBY to MBA.

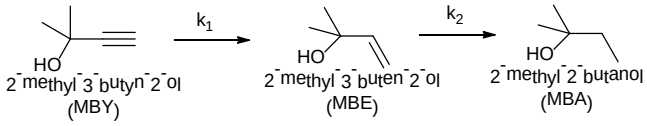

Figure 8. Scheme of 2-methyl-3-butyn-2-ol hydrogenation reactions.

The concentration profiles of the reactant and products in the MBY hydrogenation over the 2 wt. % Pd/ZnO catalyst in the batch reactor are shown in Figure 9. The concentration profiles were modelled using the Langmuir-Hinshelwood kinetics with competitive adsorption of organic species and dissociated hydrogen on the catalyst surface with the rate equation 3-5 [54,55]. Considering vapour pressure of MBY of 0.27 bar at the reaction temperature, hydrogen pressure (P_{H2}) in the system was taken as 0.73 bar.

$$r_1 = \frac{k_1^* C_{MBY}\ p_{H2}}{(Q_1\ C_{MBE} + C_{MBY} + Q_2 C_{MBA})^2} \quad (3)$$

$$r_2 = \frac{k_2^*\ C_{MBE}\ p_{H2}}{(Q_1\ C_{MBE} + C_{MBY} + Q_2 C_{MBA})^2} \quad (4)$$

$$r_3 = \frac{k_3^*\ C_{MBY}\ p_{H2}^2}{(Q_1\ C_{MBE} + C_{MBY} + Q_2 C_{MBA})^2} \quad (5)$$

where C_{MBY}, C_{MBE} and C_{MBA} are the concentrations of the organic species, k^*_1-k^*_3 are the apparent rate constants of the corresponding reaction steps, $Q_1=K_{MBE}/K_{MBY}$, $Q_2=K_{MBA}/K_{MBY}$ are the ratios of adsorption constants.

The rate equations (Eqs. 3-5) were solved numerically in the Matlab software using a Runge-Kutta method optimised for stiff systems of ordinary differential equations (ode23tb solver). The regression analysis was performed using a non-linear weighted least squares routine using Levenberg-Marquardt with the statistical weights reciprocal to the experimental uncertainties. The error analysis of the kinetic parameters was performed using a Monte-Carlo method analysing results on 2000 data sets with the initial data normally distributed around the experimental results [56].

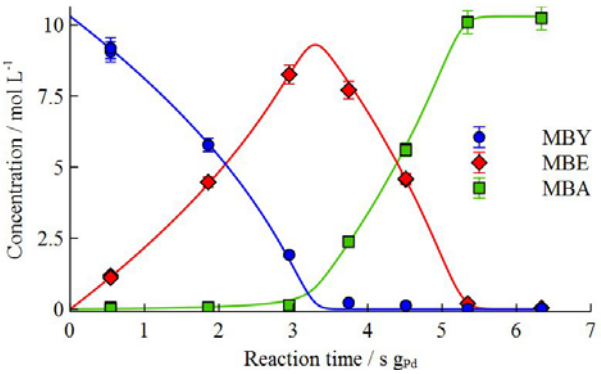

Figure 9. Concentration profiles of solvent-free MBY hydrogenation in a batch reactor on the 2. % Pd/ZnO reference catalyst at 70 C and ambient H_2 pressure. Curves present results of kinetic modelling.

The obtained constants are listed in Table 1. The values of k_2^* and k_3^* are more than 100 times lower than k_1^* value which explains the very high MBE selectivity observed in Figure 9. The k_3^* rate constant has wide confidence intervals and demonstrates that the experimental data can be accurately described considering only two consecutive reaction stages. This result is in line with the data reported for Pd and Pd-Bi catalysts [54,55]. The K_{MBE}/K_{MBY} and K_{MBA}/K_{MBY} ratios are below 0.1. This result agrees with previously published data reporting preferential adsorption of alkynes on Pd catalysts which is another factor contributing to the high alkene selectivity [57,58].

Table 1. Kinetic parameters for MBY hydrogenation obtained by regression analysis of experimental data

Parameter	Unit	value	68 % c.i.	95% c. i.
k_1^*	mol L^{-1} s^{-1} g^{-1}_{Pd} bar^{-1}	2.71×10^{1}	$(2.68 – 2.79) \times 10^{1}$	$(2.59 – 2.90) \times 10^{1}$
k_2^*	mol L^{-1} s^{-1} g^{-1}_{Pd} bar^{-1}	4.37×10^{-1}	$(3.74 – 6.33) \times 10^{-1}$	$(1.88 – 9.82 \times 10^{-1}$
k_3^*	mol L^{-1} s^{-1} g^{-1}_{Pd} bar^{-2}	1.73×10^{-1}	$(0.23 – 2.62) \times 10^{-1}$	$(0.00 – 4.02) \times 10^{-1}$
Q_1	-	9.38×10^{-2}	$(8.68 – 11.2) \times 10^{-2}$	$(6.25 – 14.3) \times 10^{-2}$
Q_2	-	1.71×10^{-2}	$(1.56 – 2.10) \times 10^{-2}$	$(1.08 – 2.71) \times 10^{-2}$

c.i. =confidence interval

3.4. Semihydrogenation in a capillary reactor

The kinetic parameters were applied to the capillary reactors and the corresponding parity plot is shown in Figure 10. There is a good agreement between the experimental data and model predictions for the r0.53 reactors, which confirms the absence of mass transfer limitations. The deviations in the area of low MBY conversions are likely caused by uncertainties in elemental analysis and variations in the dispersion of Pd nanoparticles. The experimental data obtained in the r0.53-2.4 reactor demonstrated substantial deviation from predicted values due to the presence of substantial mass transfer limitations in this reactor.

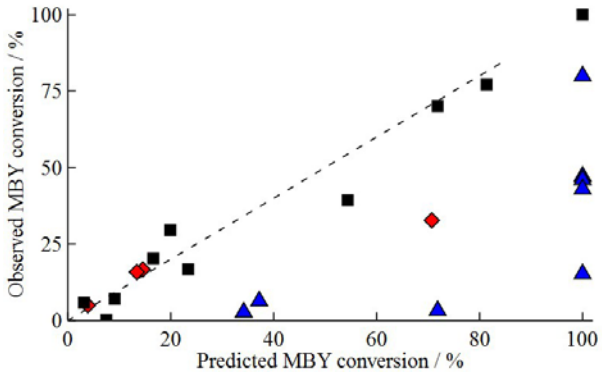

Figure 10. Parity plot for MBY conversion in the microreactors for capillary 0.53 mm i.d. microreactors (r0.53) at liquid flow rates of (■) 10 µL min^{-1} and (♦) 40 µL min^{-1}, and in 1.6 mm i.d. millireactors (r1.6) at liquid flow rate of (▲) 10 µL min^{-1}. Dashed line corresponds to perfect agreement.

For the r1.6 reactors, the picture was completely different as all the points show reaction rates much lower than that expected for the modelled conditions, i.e. without mass transfer limitations. The Weisz-Prater criterion was calculated to estimate internal mass transfer limitations of hydrogen and organic species (Eq. 6):

$$N_{W-P} = \frac{\Re\, h_c^2}{C_s\, D_{eff}} \qquad (6)$$

where $\Re$ is the apparent reaction rate, h_c is the coating thickness, C_s is the concentration of the diffusing species with the effective diffusivity of D_{eff}. Diffusivities of dissolved hydrogen and organic species of $7.0 \cdot 10^{-9}$ m^2 s^{-1} and $2.0 \cdot 10^{-9}$ m^2 s^{-1} were estimated according to Vannice [59]. A value of $N_{W-P} = 0.5$ for hydrogen in the coating with a thickness of 6 µm, indicates the presence of internal diffusion limitations. For organic species, however, diffusion limitations were highly unlikely because their concentrations, 4 orders of magnitude higher than that of hydrogen, resulted in N_{W-P} numbers below 10^{-3}. Still, at the high MBY conversion and for thick catalytic coating observed in the r1.6-1.8 reactor, N_{W-P} reached values ~1 suggesting pore limitations of MBE. Indeed, low MBE selectivity of 91 % for the r1.6-1.8 reactor indicates that pore diffusion

limitations were observed for both organic and hydrogen species. The observed linearity with Pd content in Figure 7 is likely caused by comparable intrinsic reaction and mass transfer rates under the studied conditions. Furthermore, pore diffusion limitations cannot be removed at a higher hydrogen pressure because the increase in the concentration of dissolved hydrogen will be compensated by the increased reaction rates resulting in the same Weisz-Prater numbers.

The pore limitations agree with the modelling performed by Warnier, who showed that pore diffusion limitations are observed faster than external transfer in a gas-liquid slug flow [60]. Considering the boundary value for the Weisz-Prater number of 0.3, the thickness of the catalytic layer where no hydrogen diffusion limitations are expected is 5 μm. This thickness is in excellent agreement with the experimental results, which show that mass transfer was observed for all the reactors with the thicker catalytic coating (Figure 6).

Considering good agreement of the kinetic model with experiment and the absence of mass transfer limitations for the reactors coated with 5 μm catalyst, the model was used to estimate maximum hydrogenation throughput for a range of capillary reactors of various lengths and diameters. Pressure drop in the reactors was estimated using Lockhart-Martinelli correlation [61,62] neglecting consumption of hydrogen in the reaction. The results presented in Table 2 show that at a reaction pressure of 50 bar, the throughput of about 1.5 kg day^{-1} can be reached in a 5 m reactor with a diameter of 0.5 mm operated at a pressure drop of 7 bar. Such a substantial pressure drop can be decreased by increasing the reactor diameter, allowing for longer reactors and higher throughputs reaching up to 28 kg day^{-1}. Further increase in diameter allows for even higher throughput, but the onset of external mass transfer limitations is expected under such conditions [60]. The throughput can further be increased via numbering up and increasing the operating pressure.

Table 2. Estimations of the maximum throughput and pressure drop in capillary reactors coated with 5 μm of 2.5% Pd/ZnO if no external mass transfer limitations apply.

d_{id}, mm	$L_{reactor}$, m	P_{H2}, bar	Δp_{drop}, bar	m, kg day^{-1}
0.5	5	1	0.5	0.03
0.5	5	50	7	1.5
1.5	5	50	0.8	4.7
1.5	30	50	10	28
2.5	30	50	2.2	47

4. Conclusions

Two series of capillary reactors with the internal diameters of 0.53 and 1.6 mm were wall–coated with Pd/ZnO and tested in solvent-free hydrogenation of a vitamin A precursor, 2-methyl-3-butyn-2-ol (MBY). Selectivity towards alkene was above 97.5 % in all the reactors studies, demonstrating feasibility of semihydrogenation in capillary reactors with minimal by-product formation. Correlation of the observed MBY conversion with the total Pd content in the reactors indicated that no mass transfer limitations were observed for the microreactors 0.53 mm i.d. up to about 1 $kg_{(Pd)}$ $m_{(reactor)}^{-3}$. Kinetic modelling of solvent-free MBY hydrogenation was performed in a batch reactor and the model was applied to the reactions in capillary reactors, confirming that mass transfer limitations were observed for the microreactor with the Pd loading of 2.4 $kg_{(Pd)}$ m^{-3} and all the millireactors 1.6 mm id. Calculation of the Weisz-Prater number demonstrated that internal diffusion of hydrogen was the limiting phenomena, so maximum thickness of the coating that creates negligible hydrogen pore diffusion is 5 μm. The kinetic model was used to estimate maximum throughput of a range of capillary reactors wall coated with a 5 μm layer of 2.5 wt. % Pd/ZnO catalyst considering that no external mass transfer limitations apply. The estimations showed that throughput of about 10-50 kg day^{-1} of liquid product can be achieved in a single reactor at the reaction pressure of 50 bar, while further increase is expected by numbering up and process intensification using higher temperature and pressure, microwave or radiofrequency heating.

Acknowledgments

Authors are grateful to Dr. C. Wiles for the access to her equipment, to the European Commission for an FP7 Grant for the MAPSYN Project (MAPSYN.eu No. CP-IP 309376), European Research Council (ERC) project 279867, the Russian Science Foundation (project 15-13-20015) for financial support.

References

[1] S.G. Newman, K.F. Jensen, The role of flow in green chemistry and engineering, Green Chem. 15 (2013) 1456–1472. doi:10.1039/c3gc40374b.

[2] K.F. Jensen, Microreaction engineering — is small better?, Chem. Eng. Sci. 56 (2001) 293–303. doi:10.1016/S0009-2509(00)00230-X.

[3] K. Jähnisch, V. Hessel, H. Löwe, M. Baerns, Chemistry in microstructured reactors, Angew. Chemie Int. Ed. 43 (2004) 406–46. doi:10.1002/anie.200300577.

[4] E. V. Rebrov, Use of microtechnologies for intensifying industrial processes, Theor. Found. Chem. Eng. 44 (2010) 791–799. doi:10.1134/S004057951005026X.

[5] B.P. Mason, K.E. Price, J.L. Steinbacher, A.R. Bogdan, T.D. McQuade, Greener approaches to organic synthesis using microreactor technology, Chem. Rev. 107 (2007) 2300–2318. doi:10.1021/cr050944c.

[6] V. Hessel, D. Kralisch, N. Kockmann, T. Noël, Q. Wang, Novel process windows for enabling, accelerating, and uplifting flow chemistry, ChemSusChem. 6 (2013) 746–789. doi:10.1002/cssc.201200766.

[7] V. Hessel, D. Kralisch, N. Kockmann, Novel Process Windows: Innovative Gates to Intensified and Sustainable Chemical Processes, John Wiley & Sons, 2014.

[8] D. Reay, C. Ramshaw, A. Harvey, Process Intensification: Engineering for Efficiency, Sustainability and Flexibility, Butterworth-Heinemann, 2013. http://books.google.com/books?hl=en&lr=&id=QV_U0Kbhh1UC&pgis=1 (accessed December 27, 2014).

[9] P. Watts, S.J. Haswell, The application of microreactors for small scale organic synthesis, Chem. Eng. Technol. 28 (2005) 290–301. doi:10.1002/ceat.200407124.

[10] C. Wiles, P. Watts, Continuous flow reactors: a perspective, Green Chem. 14 (2012) 38–54. doi:10.1039/c1gc16022b.

[11] D.M. Roberge, L. Ducry, N. Bieler, P. Cretton, B. Zimmermann, Microreactor Technology: A Revolution for the Fine Chemical and Pharmaceutical Industries?, Chem. Eng. Technol. 28 (2005) 318–323. doi:10.1002/ceat.200407128.

[12] B.P. Mason, K.E. Price, J.L. Steinbacher, A.R. Bogdan, D.T. McQuade, Greener approaches to organic synthesis using microreactor technology., Chem. Rev. 107 (2007) 2300–18. doi:10.1021/cr050944c.

[13] S.G. Newman, L. Gu, C. Lesniak, G. Victor, F. Meschke, L. Abahmane, et al., Rapid Wolff–Kishner reductions in a silicon carbide microreactor, Green Chem. 16 (2014) 176–180. doi:10.1039/C3GC41942H.

[14] B.J. Deadman, S.G. Collins, A.R. Maguire, Taming Hazardous Chemistry in Flow: The Continuous Processing of Diazo and Diazonium Compounds, Chem. - A Eur. J. 21 (2015) 2298–2308. doi:10.1002/chem.201404348.

[15] R.D. Chambers, M. a. Fox, G. Sandford, Elemental fluorine : Part 18. Selective direct fluorination of 1,3-ketoesters and 1,3-diketones using gas/liquid microreactor technology, Lab Chip. 5 (2005) 1132. doi:10.1039/b504675k.

[16] T.H. Rehm, Photochemical Fluorination Reactions - A Promising Research Field for Continuous-Flow Synthesis Introduction – Why fluorine ?, Chem. Eng. Technol. (2015) article ASAP 10.1002/ceat.201500195. doi:10.1002/ceat.201500195.

[17] E. V Rebrov, A. Berenguer-Murcia, A.E.H. Wheatley, B.F.G. Johnson, J.C. Schouten, Thin catalytic coatings on microreactor walls A way to make industrial processes more efficient, Chim. Oggi-Chemistry Today. 27 (2009) 4–7. <Go to ISI>://000268662700002.

[18] A.R. Dubrovskiy, E. V. Rebrov, S.A. Kuznetsov, J.C. Schouten, A microstructured reactor/heat-exchanger for the water-gas shift reaction operated in the 533-673 K range, Catal. Today. 147 (2009) 198–203. doi:10.1016/j.cattod.2009.07.037.

[19] P. V. Snytnikov, M.M. Popova, Y. Men, E. V. Rebrov, G. Kolb, V. Hessel, et al., Preferential CO oxidation over a copper-cerium oxide catalyst in a microchannel reactor, Appl. Catal. A Gen. 350 (2008) 53–62. doi:10.1016/j.apcata.2008.07.036.

[20] I.Z. Ismagilov, E.M. Michurin, O.B. Sukhova, L.T. Tsykoza, E. V Matus, M.A. Kerzhentsev, et al., Oxidation of organic compounds in a microstructured catalytic reactor, Chem. Eng. J. 135 (2008) S57–S65. doi:10.1016/j.cej.2007.07.036.

[21] I. Miguel-García, M. Navlani-García, J. García-Aguilar, Á. Berenguer-Murcia, D. Lozano-Castelló, D. Cazorla-Amorós, Capillary microreactors based on hierarchical SiO2 monoliths

incorporating noble metal nanoparticles for the Preferential Oxidation of CO, Chem. Eng. J. 275 (2015) 71–78. doi:10.1016/j.cej.2015.04.020.

[22] B. Tidona, A. Urakawa, P. Rudolf von Rohr, High pressure plant for heterogeneous catalytic CO2 hydrogenation reactions in a continuous flow microreactor, Chem. Eng. Process. Process Intensif. 65 (2013) 53–57. doi:10.1016/j.cep.2013.01.001.

[23] S. Allahyari, M. Haghighi, A. Ebadi, Direct synthesis of DME over nanostructured CuO–ZnO–Al2O3/HZSM-5 catalyst washcoated on high pressure microreactor: Effect of catalyst loading and process condition on reactor performance, Chem. Eng. J. 262 (2015) 1175–1186. doi:10.1016/j.cej.2014.10.062.

[24] B. Todić, V. V. Ordomsky, N.M. Nikačević, A.Y. Khodakov, D.B. Bukur, Opportunities for intensification of Fischer–Tropsch synthesis through reduced formation of methane over cobalt catalysts in microreactors, Catal. Sci. Technol. 5 (2015) 1400–1411. doi:10.1039/C4CY01547A.

[25] S.K. Ajmera, M.W. Losey, K.F. Jensen, M.A. Schmidt, Microfabricated packed-bed reactor for phosgene synthesis, AIChE J. 47 (2001) 1639–1647. doi:10.1002/aic.690470716.

[26] R.B.N. Baig, R.S. Varma, Magnetically retrievable catalysts for organic synthesis., Chem. Commun. 49 (2013) 752–70. doi:10.1039/c2cc35663e.

[27] T.K. Houlding, E. V. Rebrov, Application of alternative energy forms in catalytic reactor engineering, Green Process. Synth. 1 (2012) 19–31. doi:10.1515/greenps-2011-0502.

[28] L.M. Rossi, N.J.S. Costa, F.P. Silva, R. Wojcieszak, Magnetic nanomaterials in catalysis: advanced catalysts for magnetic separation and beyond, Green Chem. 16 (2014) 2906–3380. doi:10.1039/c4gc00164h.

[29] T. Zhang, X. Zhang, X. Yan, L. Kong, G. Zhang, H. Liu, et al., Synthesis of Fe3O4@ZIF-8 magnetic core-shell microspheres and their potential application in a capillary microreactor, Chem. Eng. J. 228 (2013) 398–404. doi:10.1016/j.cej.2013.05.020.

[30] A.-K. Liedtke, F. Bornette, R. Philippe, C. de Bellefon, Gas–liquid–solid “slurry Taylor” flow: Experimental evaluation through the catalytic hydrogenation of 3-methyl-1-pentyn-3-ol, Chem. Eng. J. 227 (2013) 174–181. doi:10.1016/j.cej.2012.07.100.

[31] E. V. Rebrov, G.B.F. Seijger, H.P.A. Calis, M.H.J.M. de Croon, C.M. van den Bleek, J.C. Schouten, Preparation of highly ordered single layer ZSM-5 coating on prefabricated stainless steel microchannels, Appl. Catal. A Gen. 206 (2001) 125–143. doi:10.1016/S0926-860X(00)00594-9.

[32] M.J.M. Mies, J.L.P. Van Den Bosch, E. V. Rebrov, J.C. Jansen, M.H.J.M. de Croon, J.C. Schouten, Hydrothermal synthesis and characterization of ZSM-5 coatings on a molybdenum support and scale-up for application in micro reactors, Catal. Today. 110 (2005) 38–46. doi:10.1016/j.cattod.2005.09.015.

[33] N. Cherkasov, A.O. Ibhadon, E. V. Rebrov, Novel synthesis of thick wall coatings of titania supported Bi poisoned Pd catalysts and application in selective hydrogenation of acetylene alcohols in capillary microreactors, Lab Chip. 15 (2015) 1952–1960. doi:10.1039/C4LC01066C.

[34] E. V Rebrov, A. Berenguer-Murcia, H.E. Skelton, B.F.G. Johnson, A.E.H. Wheatley, J.C. Schouten, Capillary microreactors wall-coated with mesoporous titania thin film catalyst supports, Lab Chip. 9 (2009) 503–6. doi:10.1039/b815716b.

[35] M. Faustini, B. Louis, P.A. Albouy, M. Kuemmel, D. Grosso, Preparation of Sol− Gel Films by Dip-Coating in Extreme Conditions, J. Phys. Chem. C. 114 (2010) 7637–7645. http://pubs.acs.org/doi/abs/10.1021/jp9114755 (accessed April 5, 2014).

[36] E. V Rebrov, E.A. Klinger, A. Berenguer-Murcia, E.M. Sulman, J.C. Schouten, Selective hydrogenation of 2-methyl-3-butyne-2-ol in a wall-coated capillary microreactor with a Pd25Zn75/TiO2 catalyst, Org. Process Res. Dev. 13 (2009) 991–998. http://pubs.acs.org/doi/abs/10.1021/op900085b (accessed May 20, 2013).

[37] L.N. Protasova, E. V. Rebrov, H.E. Skelton, A.E.H. Wheatley, J.C. Schouten, A kinetic study of the liquid-phase hydrogenation of citral on Au/TiO2 and Pt–Sn/TiO2 thin films in capillary microreactors, Appl. Catal. A Gen. 399 (2011) 12–21. doi:10.1016/j.apcata.2011.03.021.

[38] C.H. Hornung, B. Hallmark, M.R. Mackley, I.R. Baxendale, S.V. Ley, A Palladium Wall Coated Microcapillary Reactor for Use in Continuous Flow Transfer Hydrogenation, Adv. Synth. Catal. 352 (2010) 1736–1745. doi:10.1002/adsc.201000139.

[39] O. Muraza, E. V. Rebrov, J. Chen, M. Putkonen, L. Niinistö, M.H.J.M. de Croon, et al., Microwave-assisted hydrothermal synthesis of zeolite Beta coatings on ALD-modified borosilicate glass for application in microstructured reactors, Chem. Eng. J. 135 (2007) 117–120. doi:10.1016/j.cej.2007.07.003.

[40] M. Irfan, T.N. Glasnov, C.O. Kappe, Heterogeneous catalytic hydrogenation reactions in continuous-flow reactors., ChemSusChem. 4 (2011) 300–16. doi:10.1002/cssc.201000354.

[41] C.G. Frost, L. Mutton, Heterogeneous catalytic synthesis using microreactor technology, Green Chem. 12 (2010) 1687. doi:10.1039/c0gc00133c.

[42] B.H. Alsolami, R.J. Berger, M. Makkee, J.A. Moulijn, Catalyst Performance Testing in Multiphase Systems: Implications of Using Small Catalyst Particles in Hydrodesulfurization, Ind. Eng. Chem. Res. 52 (2013) 9069–9085. doi:10.1021/ie4010749.

[43] R. Easterday, C. Leonard, O. Sanchez-Felix, Y. Losovyj, M. Pink, B.D. Stein, et al., Fabrication of magnetically recoverable catalysts based on mixtures of Pd and iron oxide nanoparticles for hydrogenation of alkyne alcohols., ACS Appl. Mater. Interfaces. 6 (2014) 21652–60. doi:10.1021/am5067223.

[44] A. Zoabi, S. Omar, R. Abu-Reziq, Chiral Ruthenium Catalyst Immobilized within Magnetically Retrievable Mesoporous Silica Microcapsules for Aqueous Asymmetric Transfer Hydrogenations, Eur. J. Inorg. Chem. 2015 (2015) 2101–2109. doi:10.1002/ejic.201403212.

[45] C.P. Park, D.-P. Kim, A Microchemical System with Continuous Recovery and Recirculation of Catalyst-Immobilized Magnetic Particles, Angew. Chemie. 122 (2010) 6977–6981. doi:10.1002/ange.201002490.

[46] M. Ueno, T. Suzuki, T. Naito, H. Oyamada, S. Kobayashi, Development of microchannel reactors using polysilane-supported palladium catalytic systems in capillaries., Chem. Commun. (2008) 1647–9. doi:10.1039/b715259k.

[47] J. Fernández, S. Chatterjee, V. Degirmenci, E. V. Rebrov, Scale-up of an RF heated micro trickle bed reactor to a kg/day production scale, Green Process. Synth. (2015). doi:10.1515/gps-2015-0035.

[48] N.G. Patil, F. Benaskar, E. V. Rebrov, J. Meuldijk, L.A. Hulshof, V. Hessel, et al., Continuous Multitubular Millireactor with a Cu Thin Film for Microwave-Assisted Fine-Chemical Synthesis, Ind. Eng. Chem. Res. 51 (2012) 14344–14354. doi:10.1021/ie300754z.

[49] M. Al-Rawashdeh, F. Yue, N.G. Patil, T.A. Nijhuis, V. Hessel, J.C. Schouten, et al., Designing flow and temperature uniformities in parallel microchannels reactor, AIChE J. 60 (2014) 1941–1952. doi:10.1002/aic.14443.

[50] M. Al-Rawashdeh, F. Yu, T.A. Nijhuis, E. V. Rebrov, V. Hessel, J.C. Schouten, Numbered-up gas–liquid micro/milli channels reactor with modular flow distributor, Chem. Eng. J. 207-208 (2012) 645–655. doi:10.1016/j.cej.2012.07.028.

[51] M. Al-Rawashdeh, L.J.M. Fluitsma, T.A. Nijhuis, E. V. Rebrov, V. Hessel, J.C. Schouten, Design criteria for a barrier-based gas-liquid flow distributor for parallel microchannels, Chem. Eng. J. 181-182 (2012) 549–556. doi:10.1016/j.cej.2011.11.086.

[52] M. Al-Rawashdeh, J. Zalucky, C. Müller, T.A. Nijhuis, V. Hessel, J.C. Schouten, Phenylacetylene hydrogenation over [Rh(NBD)(PPh3) 2]BF4 catalyst in a numbered-up microchannels reactor, Ind. Eng. Chem. Res. 52 (2013) 11516–11526. doi:10.1021/ie4009277.

[53] R.R.E. Cable, R.E.R. Schaak, R. V September, V. Re, M. Recei, V. October, Low-temperature solution synthesis of nanocrystalline binary intermetallic compounds using the polyol process, Chem. Mater. 17 (2005) 6835–6841. http://pubs.acs.org/doi/abs/10.1021/cm0520113 (accessed July 9, 2014).

[54] Z. Wu, N. Cherkasov, G. Cravotto, E. Borretto, A.O. Ibhadon, J. Medlock, et al., Ultrasound- and Microwave-Assisted Preparation of Lead-Free Palladium Catalysts: Effects on the Kinetics of Diphenylacetylene Semi-Hydrogenation, ChemCatChem. 7 (2015) 952–959. doi:10.1002/cctc.201402999.

[55] N. Cherkasov, A.O. Ibhadon, A. McCue, J.A. Anderson, S.K. Johnston, Palladium–bismuth intermetallic and surface-poisoned catalysts for the semi-hydrogenation of 2-methyl-3-butyn-2-ol, Appl. Catal. A Gen. 497 (2015) 22–30. doi:10.1016/j.apcata.2015.02.038.

[56] J.S. Alper, R.I. Gelb, Standard errors and confidence intervals in nonlinear regression: comparison of Monte Carlo and parametric statistics, J. Phys. Chem. 94 (1990) 4747–4751. doi:10.1021/j100374a068.

[57] D. Mei, P. Sheth, M. Neurock, C. Smith, First-principles-based kinetic Monte Carlo simulation of the selective hydrogenation of acetylene over Pd(111), J. Catal. 242 (2006) 1–15. doi:10.1016/j.jcat.2006.05.009.

[58] M. García-Mota, J. Gómez-Díaz, G. Novell-Leruth, C. Vargas-Fuentes, L. Bellarosa, B. Bridier, et al., A density functional theory study of the “mythic” Lindlar hydrogenation catalyst, Theor. Chem. Acc. 128 (2010) 663–673. doi:10.1007/s00214-010-0800-0.

[59] M.A. Vannice, Kinetics of Catalytic Reactions, Springer Science+Business Media, New York, 2005. doi:10.1007/b136380.

[60] M.J.F. Warnier, Taylor flow hydrodynamics in gas-liquid-solid micro reactors, 2009.

[61] D. Chisholm, A theoretical basis for the Lockhart-Martinelli correlation for two-phase flow, Int. J. Heat Mass Transf. 10 (1967) 1767–1778. doi:10.1016/0017-9310(67)90047-6.

[62] R.W. Lockhart, R.C. Martinelli, Proposed correlation of data for isothermal two-phase, two-component flow in pipes, Chem. Eng. Prog. 45 (1949) 39–48.